

## REVIEW

# Historical overview of imaging the meibomian glands

William Ngo, Sruthi Srinivasan\*, Lyndon Jones

Centre for Contact Lens Research, School of Optometry and Vision Science, University of Waterloo, Waterloo, Ontario, Canada

Received 15 July 2012; accepted 27 September 2012

Available online 24 November 2012

### KEYWORDS

Meibomian gland;  
Imaging;  
Meibography;  
Confocal microscopy;  
OCT;  
Transillumination

**Abstract** Growing knowledge of the role of the meibomian glands in dry eye disease and contact lens discomfort has resulted in a surge of interest in visualizing these glands within the eyelids. This manuscript provides an overview of the many different visualization methods that have evolved over the past 30–40 years. Some of the visualization methods covered in this review include lid transillumination, video and non-contact meibography, and imaging methods employing confocal microscopy, optical coherence tomography and ultrasound. This review has also highlighted all the studies to date that have employed meibography as part of their methods. An overview of the available meibography dropout grading systems will also be provided.

© 2012 Spanish General Council of Optometry. Published by Elsevier España, S.L. All rights reserved.

### PALABRAS CLAVE

Glándula  
Meibomiana;  
Imagen;  
Meibografía;  
Microscopía confocal;  
OCT;  
Transiluminación

### Visión general histórica sobre la toma de imágenes de las glándulas meibomianas

**Resumen** El incremento de información sobre el papel de las glándulas meibomianas en el ojo seco y en las molestias causadas por lentes de contacto ha originado un interés creciente por visualizar dichas glándulas dentro de los párpados. Este informe aporta una visión general sobre los diferentes métodos de visualización que han ido evolucionando durante los últimos 30 a 40 años. Algunos de los métodos de visualización cubiertos por esta revisión incluyen la transiluminación del párpado, vídeo y meibografía sin contacto, y los métodos de toma de imagen que utilizan microscopía confocal, tomografía de coherencia óptica y ultrasonidos. Esta revisión ha resaltado también todos los estudios realizados hasta la fecha que han utilizado la meibografía como parte de sus métodos. Se aportará también una visión general sobre los sistemas de graduación meiógráfica abandonados, de los que se dispone.

© 2012 Spanish General Council of Optometry. Publicado por Elsevier España, S.L. Todos los derechos reservados.

\* Corresponding author at: Centre for Contact Lens Research, University of Waterloo, 200 University Avenue West, Waterloo, Ontario, N2L 3G1, Canada. Tel.: +1 519 888 4567x37311; fax: +1 519 888 4303.

E-mail address: s2srniv@uwaterloo.ca (S. Srinivasan).

## Introduction

The meibomian glands (MGs) are modified sebaceous glands that are embedded into the tarsal plate of both the superior and inferior eyelid. A MG unit contains a long central duct surrounded by grape-like structures called gland acini. These acini are filled with secretory meibocytes and connect to the central duct through ductules. These ductules deliver lipid secreted by meibocytes into the lumen of the central duct.<sup>1</sup> Upon blinking, the muscles of Riolan within the lid relax, and the orbicularis applies a compression force to these glands, causing the lipids to travel out of the orifices, which are located at the eye lid margin (Fig. 1).<sup>2</sup> The lipids play a significant role in affecting the surface tension of the tear film and slowing the evaporation rate of the tear film layer.<sup>3,4</sup> Meibomian gland dysfunction (MGD) is a disruption to this process that ultimately results in evaporative dry eye.<sup>5-7</sup> The Tear Film and Ocular Surface Society recently recommended that MGD be defined as “*a chronic, diffuse abnormality of the meibomian glands, commonly characterized by terminal duct obstruction and/or qualitative/quantitative changes in the glandular secretion. This may result in alteration of the tear film, symptoms of eye irritation, clinically apparent inflammation, and ocular surface disease*”.<sup>8</sup> There are many objective criteria by which MGD can be evaluated, including slit lamp biomicroscopy for the assessment of MG appearance, tear break up time, expressivity, or analysing meibum expressed from the glands.<sup>8</sup>

One method of evaluating the health of the MGs is termed “meibography”, which relates to various methods of visualizing and imaging the MGs. Meibography has become an important tool for both researchers trying to understand the nature of MGD and also clinicians assessing and tracking the course of the disease. There are a number of methods in which meibography can be performed, and the technique has evolved over the past few decades, with advances in medical technology. Traditionally, the eyelids were transilluminated with a light source, and the transmitted infrared (IR) rays were captured with an IR camera.<sup>9-11</sup> Newer techniques now permit observers to detect microscopic changes in the structure of MGs. This review will provide a brief history and description of each technique.

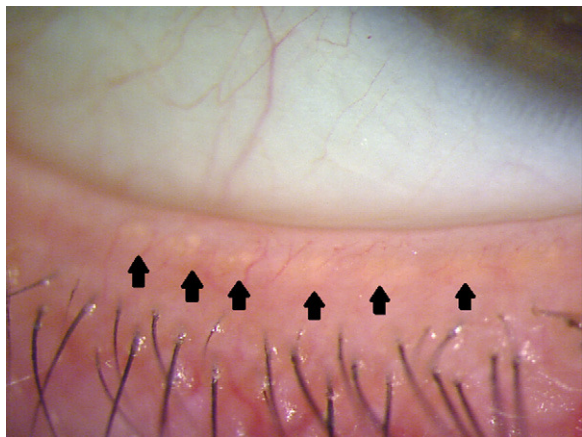


**Figure 1** Slit lamp image of the lower lid margin showing the meibomian orifices.

## Lid transillumination

The technique of transilluminating the lid and observing it under the microscope was first described by Tapie in 1977,<sup>9</sup> using an illumination probe typically used during intraocular vitreous surgery.<sup>9,10,12</sup> The tip of the probe was inserted behind the everted eyelid and the silhouette of the MG then observed on the other side. At the time, this was the only way of obtaining information about the morphology and physical characteristics of the MGs. Some major disadvantages of this technique include the fact that the probe tip is small and sharp, resulting in brightness, heat discomfort and pain reports from patients.<sup>13</sup> The transillumination area is also small, making it difficult to capture images of the entire length of the lid. A variety of light sources have been used to transilluminate the lid.<sup>13,14</sup> Areas of gland dropout in the lid are indicated by decreased transmission of light.

Fibre optic cables (Medical Research Instruments Inc., Cambridge, MA, USA) and other devices (L-3920; Inami, Co., Tokyo, Japan, MHF-C50LR; Moritex, Tokyo, Japan) have been used in studies as the light source for transillumination.<sup>12,15-19</sup> As the eyelid is everted over the fibre optic cable, it is transilluminated by the light that is conducted through the cable and, since fibre optic cables are smaller and thinner, it is more patient-friendly than solid, hand-held probes. Once the lid is transilluminated, the MGs and acini are revealed, enabling the practitioner to evaluate and record the appearance of the glands, initially via some form of photography. Meiboscopy is the viewing and assessment of the MGs (using a tool like a Finoff transilluminator) without the use of photography, whereas meibography implies visualization and the use of photography, film or digital. Meiboscopy was used to estimate gland loss in the nasal and temporal sections of the lid using a 0-3 scale.<sup>20</sup> An early study documented the use of a Zeiss photo slit-lamp with IR Kodak high-speed film (HIE 135-20 @ 1/60s, f/32).<sup>11</sup> Traditionally, the process of capturing IR images was limited to cameras with IR film; however, the process of developing IR film was very time consuming.

In the images obtained, the number of glands can be counted and the degree of gland dropout, or area of MG loss, can be measured. These two parameters have been useful as an adjunct to studies involving MGD, and lid transillumination was often used to collect this information. Numerous studies have used this technique and, in conjunction with other testing procedures, have successfully correlated MG dropout to isotretinoin use, a vitamin A analogue used for the treatment of acne vulgaris ( $n=21$ ),<sup>21</sup> blepharitis ( $n=30$ ),<sup>16</sup> chronic blepharitis ( $n=77$ ),<sup>12</sup> ageing ( $n=354$ ),<sup>19</sup> ocular surface disease and discomfort ( $n=201$ ),<sup>5</sup> and Sjögren's syndrome ( $n=27$ ).<sup>15</sup>

The practice of lid transillumination remains a key technique in studying MGs. However, the method of capturing and developing images on IR film has been replaced by more advanced digital video systems that are capable of instantaneously producing high quality images.<sup>22</sup>

## Video meibography systems

Due to the inconvenience that accompanied developing IR film, clinicians and researchers began to look for

alternative methods to perform meibography. In 1994, Mathers et al.<sup>22</sup> developed the first significant improvement to the existing technique when they developed a video-meibography system in which the transilluminated lid was viewed in real time on a computer.<sup>22</sup> The design of the transilluminator incorporated a T-shaped adapter at the head of the probe, which was used to facilitate lid eversion. The IR charge-coupled (ICC) camera is placed on the patient's visual axis and the everted lids are viewed on a video monitor. Videos were recorded to a super VHS recorder and individual frames from the video sequence were subsequently extracted for analysis.<sup>22</sup> The quality of the images captured was comparable to the images captured on an IR film camera, but without the inconvenience of developing IR film, making IR film technology obsolete. A major remaining disadvantage was that the technique still required a minimum of 5 images to encompass the entire length of the lid.<sup>22</sup>

In 1996, Matsuoka and colleagues reported the ability to capture video images of MGs using a high resolution monochromatic CCD camera and a penlight,<sup>23</sup> and Yokoi et al. modified this technique by attaching a penlight (MINI MAGLITE™, MAG INSTRUMENTS Inc., Ontario, CA, USA) to an adapter that was designed in-house.<sup>24</sup> The adapter is obliquely T-shaped, measuring 20 mm in width and 4 mm in diameter and equipped with two slit windows to transmit penlight illumination. The adapter fits over the head of the penlight, and the patients' lids can be easily everted over the adapter and transilluminated. A monochromatic CCD video camera (SSC-M420, SONY, Tokyo, Japan) records the video onto a digital video recorder (WV-D10000, SONY, Tokyo, Japan), and using computer software, the video images of the MGs can be reconstructed to form the length of the entire eyelid.<sup>24</sup>

This technique was modified further by Yokoi et al. in 2007.<sup>13</sup> The light probe was redesigned to enhance participant comfort and provide optimal lid transillumination. The head of the probe is an oblong T-shape, 20 mm wide × 3 mm in diameter to facilitate lid eversion. Running along the head of the probe are 2 rows of 8 windows (1.55 mm in size), arranged 90 degrees to each other. The IR light source consists of four IR LEDs (850 nm, 50 mW/sr) located in the body of the probe, with a 0.25 mm diameter optical fibre cable that transmits the light to the windows at the head of the probe.<sup>13</sup> The windows along the probe provide increased surface area of transillumination along the everted lid compared to the traditional probe. The shape of the probe head also allows the probe to be fitted comfortably behind the lid when everted, resulting in less discomfort for the patient.<sup>13</sup> The images are captured by an IR CCD camera (412,000 pixels; PX30B, Primetech Engineering, Tokyo, Japan) and a digital video recorder (WV-D10000, Sony, Tokyo, Japan), and computer imaging software is used to combine individual images to compose the entire length of the lid. With this improved technique, only 3 images are needed to accomplish this.<sup>13</sup>

Using this method, one study has demonstrated the effectiveness of video-meibography systems in relating giant papillary conjunctivitis to MGD ( $n=42$ ).<sup>25</sup>

With improved probe design and image processing techniques, patient discomfort has been reduced and the need for IR film has been eliminated. More recently, novel

techniques have emerged that permit meibography to be performed without using a transilluminating probe.

## Non-contact meibography

In 2008, Arita et al.<sup>26</sup> used a slit lamp (RO 5000, Rodenstock, Munich, Germany) equipped with an IR-CCD camera (XE-E150, Sony, Tokyo, Japan) combined with an IR-transmitting filter (IR-83, Hoya, Tokyo, Japan) to capture images of MGs.<sup>26</sup> This setup does not require the use of a transilluminating probe, which increases patient comfort during the acquisition of the images. This technique does not require IR light or IR film, and the MGs can be observed within a 1 min time-frame, making meibography more feasible to perform in clinical practice.<sup>26</sup>

In 2011, Pult et al.<sup>27</sup> developed a novel non-contact meibography system by modifying an IR security camera (802CHA CCD; Shenzhen LYD Technology Co. Ltd., Shenzhen, China).<sup>27</sup> The IR CCD video-camera contained an IR light source and emitted IR light towards the everted lids (Fig. 2, left); the reflected light is captured by the IR-CCD video camera and the information is sent to the computer via Video-to-FireWire Converter (The Image Source Europe GmbH, Bremen, Germany). The images were then analyzed by ImageJ 1.42q (Wayne Rasband, National Institutes of Health, Bethesda, MD, USA),<sup>27</sup> a public domain image analysis java software that offers a variety of tools to process and extract data and information from a variety of image formats.<sup>28,29</sup>

The system was adapted for near viewing by mounting a +20.00 diopter lens in front of the security camera, allowing the MGs to be viewed up-close without using a slit lamp. Using this system, Pult et al. reported on the differences in MG morphology between the upper and lower lids (Fig. 2, right).<sup>30</sup>

In 2012, Srinivasan and colleagues reported on the use of a commercially available instrument, the Keratograph 4 (OCULUS, Wetzlar, Germany and JenVis Research (Jena, Germany)) to perform meibography.<sup>31,32</sup> The Keratograph 4 primarily functions as a corneal topographer, but can also be used to undertake pupillometry, utilizing an in-built IR bulb and camera (Fig. 3, left). The participant is seated and asked to focus on the target at the centre of the placido



**Figure 2** An infrared security camera modified for meibography (left). A ring of infrared LEDs illuminate the eye, and the central camera unit captures infrared video to be displayed on a computer screen (not shown). The inferior lid is everted to reveal MGs in infrared light. This image was captured by the modified security camera. The ring configuration of the infrared LEDs of the camera can be seen in the reflection of the cornea (right).

Courtesy of Dr. Heiko Pult.

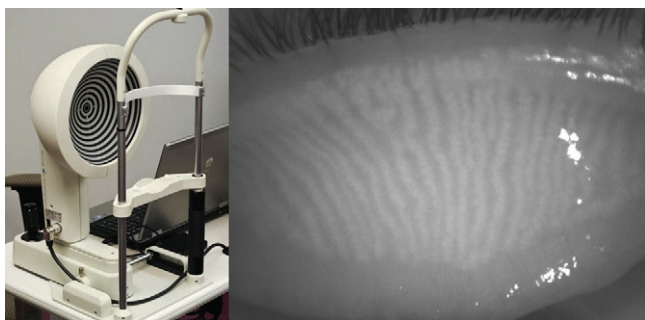


**Figure 3** The OCULUS Keratograph 4 functions primarily as a corneal topographer, however the infrared diode intended for pupillometry can be used as an infrared illumination source for meibography (left). An everted superior eyelid reveals long thin MGs running vertically on the palpebral side as visualized by the OCULUS Keratograph 4 in infrared light (right).

disc and then the lower lid is everted using a cotton-tipped applicator. The intensity of the IR illumination can be manually adjusted with software built into the device, but is kept consistent throughout the study. When observing the palpebral surface of the eyelids illuminated with IR light, the MGs are revealed and can be captured using either video or still images (Fig. 3, right).<sup>33</sup> The degree of MG dropout was determined subjectively using Arita et al.'s MG dropout score (MGDS),<sup>26</sup> and the area of dropout was digitally determined using ImageJ. The dropout scores were then compared with the Ocular Surface Disease Index (OSDI) scores obtained from the same participants, and a positive correlation was found between MGDS and OSDI scores, and increased dropout area and OSDI scores ( $n = 37$ ).<sup>33</sup> In a more recent model, the OCULUS Keratograph 5M allows for meibography-friendly features including the re-positioning of the IR diodes to minimize interfering reflections, increasing the field of view so the entire eyelid can be imaged (Fig. 4, left), and incorporating image processing that highlights the MGs (Fig. 4, right).

b o n Optic, a German ophthalmic instruments manufacturer has advertised that a few of their devices, namely the EyeTop-S corneal topographer, the Sirius Scheimpflugkamera, and the Cobra retinal camera (b o n Optic, Lübeck, Germany) are all capable of performing meibography.<sup>34–36</sup> Although little is published about these devices, there is one case report involving the use of the Sirius Scheimpflugkamera to aid in the follow-up of a MGD-symptomatic dry eye case.<sup>37</sup>

Non-contact meibography has been employed to show increased MG duct distortion in patients with perennial allergic conjunctivitis ( $n = 102$ ),<sup>38</sup> increased dropout in patients

with contact lens wear ( $n = 258$ ),<sup>39</sup> that the glands of the lower lid have an increased tendency for dropout when compared to glands within the upper lid ( $n = 20$ )<sup>30</sup> and that increased MG dropout occurs with increasing age ( $n = 236$ ).<sup>26</sup> This method has also been used to assess the reliability of meibography grading scales ( $n = 290$ ),<sup>18</sup> provide diagnostic parameters for obstructive and seborrheic MGD ( $n = 113$ ),<sup>40,41</sup> and differentiating between obstructive MGD and aqueous deficient dry eye ( $n = 40$ ).<sup>42</sup>

Despite the different methods available to undertake meibography, they all provide a gross view of the MGs and allow observers to make observations and monitor MG dropout and morphological distortion. More detailed information about MGs and MGD can be obtained by examining them under higher magnification. Previously, studying the ultrastructure of MGs required preparing and viewing histological sections belonging to animal models or from human exenterations,<sup>11,43,44</sup> but with advances in imaging technology it is now possible to view the ultrastructure of human MGs in vivo using a variety of anterior segment observational instruments.<sup>14,45–56</sup>

### Confocal microscopy

The HRT II with Rostock Cornea Module (Heidelberg Engineering GmbH, Dossenheim, Germany) uses a 670 nm LED light to provide high resolution scans (optical:  $4 \mu\text{m}$  horizontally,  $2 \mu\text{m}$  vertically, digital:  $1 \mu\text{m}/\text{pixel}$  vertically and horizontally) of biological tissue. The images generated at  $384 \times 384$  pixels correspond to a  $400 \times 400 \mu\text{m}$  field of view, and can be analyzed with the built-in software, or with ImageJ.<sup>46,52,53</sup>

The Rostock Cornea Module is mounted onto the objective tube of the laser scanning camera, and a large drop of highly viscous gel (i.e. GenTeal® Comfort Gel) is applied to the front of the microscope lens. A sterile plastic cap (the TomoCap) is mounted on its holder to cover the microscope lens. The cap serves to secure the viscous gel onto the lens, in addition to acting as an applanating surface that contacts the eye. The focal plane of the instrument is adjusted to the outer surface of the TomoCap.<sup>45,52,53</sup> Topical anaesthetic is applied to the eye and the participant is seated with the head properly aligned on the head rest. The eyelids are then everted and the TomoCap is held against the palpebral conjunctiva, and scanning then begins.<sup>45,52,53</sup>

The first group to use confocal microscopy to observe the palpebral conjunctiva was Kobayashi et al. in 2005,<sup>48</sup> who reported that the instrument was able to resolve the cells of the conjunctiva. Furthermore, “web-like structures” were

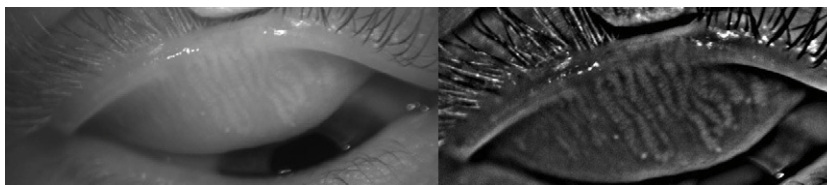


**Figure 4** The entire superior palpebral surface could be imaged using the OCULUS Keratograph 5M (left). A processed image of the same eyelid highlights the MGs to make them more visible (right).

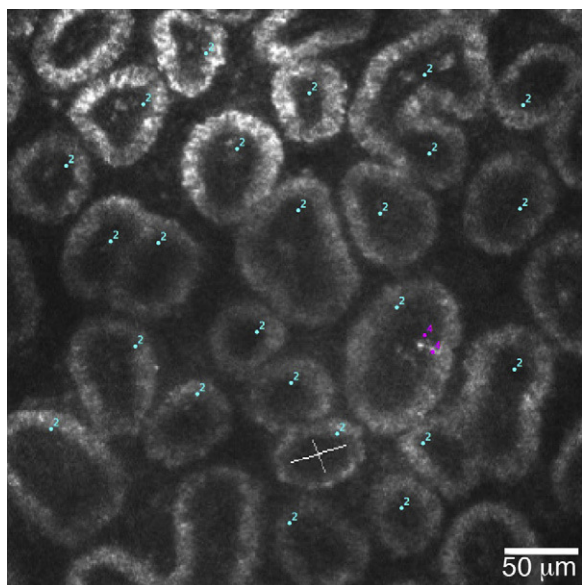


**Figure 5** A 400  $\mu\text{m} \times 400 \mu\text{m}$  frame of acini clusters as seen with the HRT-II Rostock Cornea Module. Acini units (cyan) and inflammatory cells (magenta) are manually marked, and density for each is automatically calculated using the Cell Count<sup>®</sup> software (Heidelberg Engineering GmbH, Germany).  
Courtesy of Dr. Murat Dogru.

seen below the conjunctiva layers, which were presumed to be MGs ( $n=4$ ).<sup>48</sup>

The primary advantage of this technique is that it allows in vivo real-time viewing of MG acini structures in microscopic detail, allowing the researcher to observe the pathology of MGD. Meibomian gland acinar unit density (MGAUD) is measured using the HRT internal software and studies have shown that loss of glandular acini density has been correlated with MGD.<sup>52,53</sup> Meibomian gland acinar longest and shortest diameter (MGALD, MGALSD) is also a useful outcome variable measured with this technique, since acini dilatation results from increased pressure due to gland obstruction.<sup>52,53</sup> Periglandular inflammatory cell density (ICD) also provides information on the severity of MGD, as blepharitis and inflammation typically accompanies this condition.<sup>52</sup>

These physical parameters provide a sensitivity ranging from 81% (MGALD) to 100% (ICD), and a specificity ranging from 81% (MGALD) to 100% (ICD) in diagnosing MGD ( $n=46$ ),<sup>52</sup> the parameters correlated well with MGD severity and the

method has proven very useful in evaluating MGD ( $n=35$ ).<sup>53</sup> This technique was used to show the effectiveness of various MGD treatment modalities ( $n=32$ ),<sup>14</sup> the effect of ageing on conjunctival and MG structures ( $n=49$ ),<sup>54</sup> the difference in morphology of gland structures between non-contact lens and contact lens wearers ( $n=40$ ),<sup>55</sup> and was able to reveal morphological changes in patients with Sjögren's syndrome ( $n=70$ ).<sup>56</sup>

There are a few other instruments that have been adapted for anterior segment use and have been successful in imaging the MGs in great detail. While they have not been widely used, they offer a different perspective on visualizing the MGs (Fig. 5).

## Optical coherence tomography

To date, the use of optical coherence tomography (OCT) to image MG structures is uncommon; however, in 2010, Bizheva et al.<sup>47</sup> were able to show the advantages of using an OCT to generate 3D and volumetric images. The images generated had dimensions of  $1000 \times 512 \times 256$  pixels, which correspond to physical dimensions of  $4 \text{ mm} \times 1 \text{ mm} \times 2 \text{ mm}$ .<sup>47</sup> The ultra-high resolution OCT provides  $3 \mu\text{m}$  axial and  $10 \mu\text{m}$  lateral resolution in biological tissue, at 91,111 A-scans/s. Although this technique allows non-invasive imaging of glands, the scan depth is limited to approximately 1–2 mm due to scattering and absorption of light by biological tissue. The design of the OCT is based on a compact fibre-optic Michelson interferometer, connected to a diode (SLD; Superlum Ltd.;  $\lambda_c = 1020 \text{ nm}$ ,  $\Delta\lambda = 110 \text{ nm}$ ). An optical imaging probe consisting of 3 achromat lenses and a pair of galvanometric sensors is connected to the sample arm, and is mounted on to a modified slit lamp. A custom high performance spectrometer (P&P Optica, Inc.), interfaced to a 1024 pixel linear array InGaAs camera (SUI, Goodrich Corp.) with 92 kHz readout rate, detects the interference signal. The signal detection quality is 99 dB SNR for 1.3 mW power of the imaging beam. The images captured by this OCT are processed by MATLAB (Mathworks) and Amira (Visage Imaging, Inc.).<sup>47</sup>

The authors were able to use the instrument to successfully obtain images ( $n=1$ ) of the main duct of the MG, in addition to clusters of acini associated with the gland (Fig. 6). They were also able to acquire images of a clinically diagnosed chalazion, which appeared as a highly reflective mass surrounded by an optically clear fluid.<sup>47,50</sup>

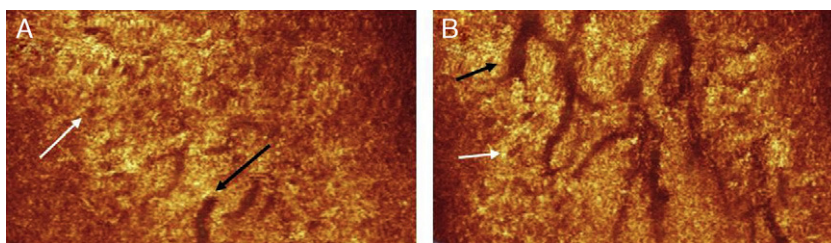


**Figure 6** A coronal section through the eyelids reveals the branch structure of the ductules of the MGs (black arrows). The acini (white arrows) appear as brown circular structures adjacent to the ductules.

Courtesy of Dr. Kostadinka Bizheva, Dr. Luigina Sorbara, Dr. Natalie Hutchings, and Dr. Trefford Simpson.

## Ultrasound

Peyman et al.<sup>51</sup> have recently reported imaging MGs using the Vevo 2100, an ultrasound device (VisualSonics, Toronto, Canada) originally intended for small animal studies. The Vevo 2100 instrument can be equipped with a variety of transducers to allow the researcher to select an appropriate field of view and resolution for specific applications. In this study, coupling gel was applied to the eyelid of a single human volunteer, and the eyelid was examined using a 50-MHz probe (MS550D, VisualSonics, Toronto, Canada).<sup>51</sup> The 50-MHz probe produced high resolution images (approximately 30  $\mu\text{m}$ ) of the coronal and transverse image planes of the eyelid. The MGs were revealed as dark spots surrounded by grey-white sonically denser material. This technique offers a unique method of imaging human MGs in vivo, but to-date there is only one paper published.<sup>51</sup>

## Meibography grading scales

Currently, there are no agreed and established standards to grade MG dropout. To-date, only one study has looked at within-reader and between-reader reliability comparing two different methods of grading MG images (gestalt scale versus individual gland counting). The authors of this study found that for both grading methods, within-reader reliability was moderate and between-reader reliability was fair ( $n = 290$ ). Nichols et al.<sup>18</sup> used both simple and weighted  $K$  statistics to examine within- and between-reader reliability of the grading scales and have used the definition of moderate to be  $0.41 < K < 0.60$  and fair to be  $0.21 < K < 0.40$ .<sup>18</sup> The authors of other studies have devised a number of ways to grade the severity of gland dropout.

Mathers et al.<sup>21</sup> graded dropout as follows:

The central 10 glands of the inferior tarsus were photographed and graded based on how much light was transmitted through the gland. Jester et al.<sup>11</sup> found that more severe dropout corresponded with decreased transmission of light, due to increased thickness of the keratinized epithelium.

- Grade 1: Normal gland
- Grade 2: Gland visible with decreased absorption
- Grade 3: Acini of gland severely atrophic with duct still visible
- Grade 4: No gland structures visible

Den et al.<sup>19</sup> graded dropout as follows:

- Grade 0: absent
- Grade 1: present (more than half of lower lid)

Arita et al.<sup>26</sup> graded dropout as follows:

- Grade 0: no dropout
- Grade 1: dropout of less than 1/3 of total area of glands
- Grade 2: dropout of more than 1/3, but less than 2/3 of total area of glands
- Grade 3: dropout of more than 2/3 of total area of glands

McCulley et al.<sup>57</sup> and Aronowicz et al.<sup>57,58</sup> graded as follows:

The central 7 glands of the tarsal plate were examined. Each gland is given a score from 0 to 4, where 0 represents no dropout, and 4 is complete dropout of that single gland. The score from each gland is summed up as a total out of 28. 0/28 would represent no dropout whereas 28/28 is complete dropout.

Shimazaki et al.<sup>15</sup> and Goto et al.<sup>15,17</sup> graded dropout as follows:

- Grade 0: no dropout
- Grade 1: loss of less than half the glands in inferior tarsus
- Grade 2: loss of more than half the glands in inferior tarsus

McCann et al.<sup>16</sup> graded dropout as follows:

Grading was based on the percentage of glands that were absent. For example, if 50% of glands had dropped out, dropout would be graded as 0.5.

Pult et al.<sup>27</sup> graded dropout as follows:

Using ImageJ to analyze photos, the area of dropout was subjectively defined and expressed as a percentage of the total area of the tarsal plate. The angles at which the glands are bent are also analyzed.

Srinivasan et al.<sup>33</sup> utilized both Arita et al.<sup>26</sup> meiboscores and digital grading systems in analyzing images, but in addition also indicated the presence or absence of white patches (to indicate acini changes), and gland tortuosity.<sup>26,27,33</sup>

Currently there is no consensus on the number of increments that should be present in a grading scale for meibography; however, Bailey et al.<sup>59</sup> have recommended that a scale of fine clinical sensitivity should not exceed one-third of the standard deviation of the discrepancy, and this implies the use of scales with smaller increments to increase the ability to detect clinical changes.<sup>59,60</sup>

## Conclusion

Meibography is a tool that can easily provide information on the severity of MGD and, with advancements in imaging technology, the MGs can now be viewed in great detail. In addition, meibography can be performed easily, quickly, and non-invasively, making it a very practical test to perform in a clinical practice setting.

Meibography correlates very well with other dry eye tests and plays an integral part in the evaluation of dry eye. It is also not uncommon to have meibography paired with other methods of imaging the MG, as they provide two different perspectives on the morphology and structure of MGs. There are varying methods to grade MG dropout and distortion and while most authors have developed their own method of grading, some have opted to use another author's grading system. However, currently, there is still no unified grading system for MG dropout and further work in this area would be valuable.

## Conflict of interest

The authors have no conflicts of interest to declare.

## Acknowledgement

The authors would like to thank Drs. Heiko Pult, Murat Dogru, Kostadinka Bizheva, Luigina Sorbara, Trefford Simpson and Natalie Hutchings for their generosity in providing images for this article.

## References

- Knop N, Knop E. Meibomian glands. Part I. Anatomy, embryology and histology of the Meibomian glands. *Ophthalmologie*. 2009;106:872–883.
- Knop E, Knop N, Millar T, Obata H, Sullivan DA. The international workshop on meibomian gland dysfunction: report of the subcommittee on anatomy, physiology, and pathophysiology of the meibomian gland. *Invest Ophthalmol Vis Sci*. 2011;52:1938–1978.
- Nagyova B, Tiffany JM. Components responsible for the surface tension of human tears. *Curr Eye Res*. 1999;19:4–11.
- Craig JP, Tomlinson A. Importance of the lipid layer in human tear film stability and evaporation. *Optom Vis Sci*. 1997;74:8–13.
- Shimazaki J, Sakata M, Tsubota K. Ocular surface changes and discomfort in patients with meibomian gland dysfunction. *Arch Ophthalmol*. 1995;113:1266–1270.
- Bron AJ, Tiffany JM. The contribution of meibomian disease to dry eye. *Ocul Surf*. 2004;2:149–165.
- Mathers WD. Ocular evaporation in meibomian gland dysfunction and dry eye. *Ophthalmology*. 1993;100:347–351.
- Nelson JD, Shimazaki J, Benitez-del-Castillo JM, et al. The international workshop on meibomian gland dysfunction: report of the definition and classification subcommittee. *Invest Ophthalmol Vis Sci*. 2011;52:1930–1937.
- Tapie R. Etude biomicroscopique des glandes de meibomius. *Ann Ocul*. 1977;210:637–648.
- Robin JB, Jester JV, Nobe J, Nicolaides N, Smith RE. In vivo transillumination biomicroscopy and photography of meibomian gland dysfunction. A clinical study. *Ophthalmology*. 1985;92:1423–1426.
- Jester JV, Rife L, Nii D, Luttrull JK, Wilson L, Smith RE. In vivo biomicroscopy and photography of meibomian glands in a rabbit model of meibomian gland dysfunction. *Invest Ophthalmol Vis Sci*. 1982;22:660–667.
- Mathers WD, Shields WJ, Sachdev MS, Petroll WM, Jester JV. Meibomian gland dysfunction in chronic blepharitis. *Cornea*. 1991;10:277–285.
- Yokoi N, Komuro A, Yamada H, Maruyama K, Kinoshita S. A newly developed video-meibography system featuring a newly designed probe. *Jpn J Ophthalmol*. 2007;51:53–56.
- Matsumoto Y, Shigeno Y, Sato EA, et al. The evaluation of the treatment response in obstructive meibomian gland disease by in vivo laser confocal microscopy. *Graefes Arch Clin Exp Ophthalmol*. 2009;247:821–829.
- Shimazaki J, Goto E, Ono M, Shimmura S, Tsubota K. Meibomian gland dysfunction in patients with Sjögren syndrome. *Ophthalmology*. 1998;105:1485–1488.
- McCann LC, Tomlinson A, Pearce EI, Diaper C. Tear and meibomian gland function in blepharitis and normals. *Eye Contact Lens*. 2009;35:203–208.
- Goto E, Monden Y, Takano Y, et al. Treatment of non-inflamed obstructive meibomian gland dysfunction by an infrared warm compression device. *Br J Ophthalmol*. 2002;86:1403–1407.
- Nichols JJ, Berntsen DA, Mitchell GL, Nichols KK. An assessment of grading scales for meibography images. *Cornea*. 2005;24:382–388.
- Den S, Shimizu K, Ikeda T, Tsubota K, Shimmura S, Shimazaki J. Association between meibomian gland changes and aging, sex, or tear function. *Cornea*. 2006;25:651–655.
- Pflugfelder SC, Tseng SC, Sanabria O, et al. Evaluation of subjective assessments and objective diagnostic tests for diagnosing tear-film disorders known to cause ocular irritation. *Cornea*. 1998;17:38–56.
- Mathers WD, Shields WJ, Sachdev MS, Petroll WM, Jester JV. Meibomian gland morphology and tear osmolarity: changes with Accutane therapy. *Cornea*. 1991;10:286–290.
- Mathers WD, Daley T, Verdick R. Video imaging of the meibomian gland. *Arch Ophthalmol*. 1994;112:448–449.
- Matsuoka T, Tsumura T, Ueda H, Hasegawa E. Video-meibographic observations of the meibomian gland. *Jpn J Clin Ophthalmol*. 1996;50:351–354.
- Yokoi N, Komuro A, Maruyama K, Kinoshita S. New instruments for dry eye diagnosis. *Semin Ophthalmol*. 2005;20:63–70.
- Mathers WD, Billborough M. Meibomian gland function and giant papillary conjunctivitis. *Am J Ophthalmol*. 1992;114:188–192.
- Arita R, Itoh K, Inoue K, Amano S. Noncontact infrared meibography to document age-related changes of the meibomian glands in a normal population. *Ophthalmology*. 2008;115:911–915.
- Pult H, Riede-Pult BH. Non-contact meibography: keep it simple but effective. *Cont Lens Anterior Eye*. 2012;35:77–80.
- Rasband WS. *ImageJ*. 2012. <http://imagej.nih.gov/ij/>
- Schneider CA, Rasband WS, Eliceiri KW. NIH image to ImageJ: 25 years of image analysis. *Nat Methods*. 2012;9:671–675.
- Pult H, Riede-Pult BH, Nichols JJ. Relation between upper and lower lids' meibomian gland morphology, tear film, and dry eye. *Optom Vis Sci*. 2012;89:310–315.
- Srinivasan S, Menzies K, Sorbara L, Jones L. Meibography of the upper lid. *Optician*. 2011:12–14, [opticianonline.net](http://opticianonline.net).
- Srinivasan S, Sorbara L, Jones L, Sickenberger W. Imaging the structure of the meibomian glands. *Contact Lens Spectrum*. 2011;(July):52–53 [www.clspectrum.com](http://www.clspectrum.com)
- Srinivasan S, Menzies K, Sorbara L, Jones L. Infra-red imaging of meibomian gland structure using a novel keratograph. *Optom Vis Sci*. 2012;89:788–794.
- bonOptic. *b o n EyeTop-S Corneal Topography System*. 2011:1–2. <http://www.bon.de/eyetops-corneal-topography-fitting-p-379.html>
- bonOptic. *b o n SIRIUS Scheimpflug-Camera*. 2011:1–4. <http://www.bon.de/sirius-scheimpflugcamera-p-481.html>
- bonOptic. *b o n COBRA Non-mydratic Digitale Fundus Camera*. 2011:1–4. <http://www.bon.de/cobra-nonmydratic-digitale-fundus-camera-p-538.html>
- Pult H, Riede-Pult B. Non-contact meibography in diagnosis and treatment of non-obvious meibomian gland dysfunction. *J Optom*. 2011;5:2–5.
- Arita R, Itoh K, Maeda S, et al. Meibomian gland duct distortion in patients with perennial allergic conjunctivitis. *Cornea*. 2010;29:858–860.
- Arita R, Itoh K, Inoue K, Kuchiba A, Yamaguchi T, Amano S. Contact lens wear is associated with decrease of meibomian glands. *Ophthalmology*. 2009;116:379–384.
- Arita R, Itoh K, Maeda S, et al. Proposed diagnostic criteria for obstructive meibomian gland dysfunction. *Ophthalmology*. 2009;116:2058–2063.
- Arita R, Itoh K, Maeda S, et al. Proposed diagnostic criteria for seborrheic meibomian gland dysfunction. *Cornea*. 2010;29:980–984.
- Arita R, Itoh K, Maeda S, Maeda K, Tomidokoro A, Amano S. Efficacy of diagnostic criteria for the differential diagnosis between obstructive meibomian gland dysfunction and aqueous deficiency dry eye. *Jpn J Ophthalmol*. 2010;54:387–391.

43. Jester JV, Nicolaides N, Smith RE. Meibomian gland studies: histologic and ultrastructural investigations. *Invest Ophthalmol Vis Sci.* 1981;20:537–547.
44. Sirigu P, Shen RL, Pinto da Silva P. Human meibomian glands: the ultrastructure of acinar cells as viewed by thin section and freeze–fracture transmission electron microscopies. *Invest Ophthalmol Vis Sci.* 1992;33:2284–2292.
45. Heidelberg. *Rostock Cornea Module—Quick Operation Notes.* 2012:1–2. <http://www.heidelbergengineering.com/us/wp-content/uploads/97097-rcmquickusernotes.031605.pdf> [accessed 2012].
46. Heidelberg. *Confocal Laser Microscopy.* 2005:1–6. <http://www.heidelbergengineering.com/wp-content/uploads/665-hrt-rostock-cornea-module.pdf>
47. Bizheva K, Lee P, Sorbara L, Hutchings N, Simpson T. In vivo volumetric imaging of the human upper eyelid with ultrahigh-resolution optical coherence tomography. *J Biomed Opt.* 2010;15:040508.
48. Kobayashi A, Yoshita T, Sugiyama K. In vivo findings of the bulbar/palpebral conjunctiva and presumed meibomian glands by laser scanning confocal microscopy. *Cornea.* 2005;24:985–988.
49. Efron N, Al-Dossari M, Pritchard N. In vivo confocal microscopy of the palpebral conjunctiva and tarsal plate. *Optom Vis Sci.* 2009;86:E1303–E1308.
50. Sorbara L, Maram J, Bizheva K, Hutchings N, Simpson TL. Case report: chalazion and its features visualized by ultrahigh resolution optical coherence tomography. *Cont Lens Anterior Eye.* 2011;34:87–91.
51. Peyman GA, Ingram CP, Montilla LG, Witte RS. A high-resolution 3D ultrasonic system for rapid evaluation of the anterior and posterior segment. *Ophthalmic Surg Lasers Imaging.* 2012:1–9.
52. Ibrahim OM, Matsumoto Y, Dogru M, et al. The efficacy, sensitivity, and specificity of in vivo laser confocal microscopy in the diagnosis of meibomian gland dysfunction. *Ophthalmology.* 2010;117:665–672.
53. Matsumoto Y, Sato EA, Ibrahim OM, Dogru M, Tsubota K. The application of in vivo laser confocal microscopy to the diagnosis and evaluation of meibomian gland dysfunction. *Mol Vis.* 2008;14:1263–1271.
54. Wei A, Hong J, Sun X, Xu J. Evaluation of age-related changes in human palpebral conjunctiva and meibomian glands by in vivo confocal microscopy. *Cornea.* 2011;30:1007–1012.
55. Villani E, Ceresara G, Beretta S, Magnani F, Viola F, Ratiglia R. In vivo confocal microscopy of meibomian glands in contact lens wearers. *Invest Ophthalmol Vis Sci.* 2011;52:5215–5219.
56. Villani E, Beretta S, De Capitani M, Galimberti D, Viola F, Ratiglia R. In vivo confocal microscopy of meibomian glands in Sjögren's syndrome. *Invest Ophthalmol Vis Sci.* 2011;52:933–939.
57. McCulley JP, Shine WE, Aronowicz J, Oral D, Vargas J. Presumed hyposecretory/hyperevaporative KCS: tear characteristics. *Trans Am Ophthalmol Soc.* 2003;101:141–152 [discussion 152–144].
58. Aronowicz JD, Shine WE, Oral D, Vargas JM, McCulley JP. Short term oral minocycline treatment of meibomianitis. *Br J Ophthalmol.* 2006;90:856–860.
59. Bailey IL, Bullimore MA, Raasch TW, Taylor HR. Clinical grading and the effects of scaling. *Invest Ophthalmol Vis Sci.* 1991;32:422–432.
60. Tomlinson A, Bron AJ, Korb DR, et al. The international workshop on meibomian gland dysfunction: report of the diagnosis subcommittee. *Invest Ophthalmol Vis Sci.* 2011;52:2006–2049.